Proceedings of the 9th International Conference of Control Systems, and Robotics (CDSR'22)
Niagara Falls, Canada – June 02-04, 2022
Paper No. 108
DOI: 10.11159/cdsr22.108

Optimal Design of a Cable-driven Wrist Prosthetic Device

J.D. Sanjuan[1,3], Md Samiul Haque Sunny[2], Jawher Ghommam[4], Brahim Brahmi[5], Inga Wang[6], Mohammad H. Rahman[1]
[1]Department of Mechanical Engineering, University of Wisconsin-Milwaukee, Milwaukee, United States
[2]Department of Computer Science, University of Wisconsin-Milwaukee, Milwaukee, United States
[3]Departamento de Ingeniería Mecánica, Universidad del Norte, Barranquilla, Colombia
[4]Departament of Electrical and Computer Engineering, Sultan Qaboos University, Al Khoudh, Oman
[6]Department of Rehabilitation Sciences & Technology, University of Wisconsin-Milwaukee, Milwaukee, United States
[5]Department of Electrical and Computer Engineering, Miami University, Oxford, United States
jsanjuan@uwm.edu; msunny@uwm.edu; brahmib@miamioh.edu; jawher@squ.edu.om; wang52@uwm.edu, rahmanmh@uwm.edu

Abstract **-** The amputation of a limb is a disabling condition that affects millions of people worldwide. This situation bolsters the necessity of devices that help the integration of those individuals into society. However, the design of such mechanisms faces many issues for their simple implementation, such as the reduced space to add actuators while maintaining an aesthetical design. This situation increases the complexities of manufacturing high dexterity upper arm prostheses. Thus, a cable-driven wrist prosthesis (CDWP) is proposed to solve these issues. Besides, the Anti-Parallel-based local Transmission Index is presented as a performance index to optimize the device's dimensions. Ultimately, by applying the methodology proposed in this article, researchers would be able to dimension the proposed CDWP for a wide range of patients.

Keywords**:** Cable-driven parallel robots; Wrist prosthesis; Performance index; Parallel robots

1. Introduction

Upper limb amputation is the removal of any part of the forearm or arm. Only in the United States, this condition affects approximately 41,000 citizens [1, 2]. Besides, according to the results of Ziegler-Graham K. et al., this value may double by 2050 [3]. Thus, continuous efforts have led to the design of high dexterity terminal devices that imitate the movement of the human hand [4]. However, in comparison, little work has been done in developing prosthetic wrists, despite the important role of this joint in manipulation tasks [5, 6]. Furthermore, some researchers allegate that increasing the agility of prosthetic wrists may serve amputees better than a highly dexterous hand, mainly because of the reduction of complications occasioned from the compensatory body motions [7]. However, besides the apparent need for the implementation of active wrist mechanisms in prostheses, its utilization faces numerous issues. One of the main concerns that limit the utilization of wrist prostheses is the additional length resulting from the integration of a wrist system [8]. Although it is possible to reduce the forearm socket length to accommodate the extra space of the wrist, this is only applicable to amputees with relatively short residual limbs (proximal amputation) [9]. Another source of concern is the additional weight from a prosthesis, which can create discrepancies between limbs that impact coordination and aesthetics [10]. Ultimately, those two issues may result in the abandonment of part of the prosthesis user [11].

Diverse prostheses were found in the literature presenting issues related to their lengths and weights [8]. To name a few, Mahmoud R. et al. designed a three degree of freedom prosthesis actuated with three servo motors [12]. However, because of the use of serial chains, the system requires large space within the wrist socket. Other approaches use parallel robots to control the wrist as a spherical joint [13-15]. But, to increase their workspace, parallel robots require to increase their size, making them heavy and bulky. Thus, researchers have proposed the implementation of cable-driven parallel robots (CDPR) to minimize the size and weight of actuated wrist prostheses. In this context, Takeda H. et al. built a system of gears actuated by motors attached to a pulley transmission [16]; Controzzi M. et al. utilizes a differential mechanism (Bevel gears) actuated by Bowden cables [17]. However, those mechanisms also present various disadvantages. For example, the former mechanism uses idle pulleys to maintain the tension and change the orientation of the cables, which increases the bulkiness of the system [18, 19]. The latter requires the utilization of special mechanisms to maintain the antagonistic forces that fix the position of the wrist, thus, adding additional requirements of torque to the actuators because of the high friction [20-22]. Nonetheless, Mustafa S. K. et al. developed a light 3-DOF wrist prosthesis using a motorized reel attached to anchor points[23]. However, the mechanism does not require a wide space within the wrist socket and is relatively light. It has unavoidable singularities because of the pronation/supination movements. Therefore, the design of a wrist prosthesis that overcomes the space and weight problems is still an open research problem.

This research presents the optimal design of a cable-driven wrist prosthesis (CDWP) using performance indexes. Performance indexes are a well-known strategy for designing parallel robots, and many authors have proposed different indexes to analyze different mechanisms [24-26]. However, in the case of cable-driven robots, the utilization of this approach has been overlooked [27, 28]. Therefore, the following work proposes a performance index for the design of CDPRs based on the computations of anti-parallel vectors. Anti-parallel vectors are parallel vectors that point to opposite directions. E.g., consider a CDPR that is required to move in the positive or negative direction of the x-axis. The wrench feasible generated by the cables requires components in both directions of the x-axis. Thus, the obtained pair of components are a pair of anti-parallel vectors. This concept is extended to the axes of motion of the end-effector to define the Anti-Parallel based local Transmission Index (APLTI), which is used for the optimal design of the CDWP through the implementation of genetic algorithms (GA).

This study is organized in the following order: Section 2 presents the description of the mechanism, including the inverse kinematics. Section 3 defines the APLTI and implementation for different cable-driven parallel robots. Then, section 4 shows the results of the optimization of the CDWP. Finally, section 5 presents the conclusions of this research.

2. Mechanism Description

The proposed CDWP is a 3SPU-U parallel robot that uses cables for actuation. The S stands for spherical, P is for prismatic and the U for universal, and each kinematical chain SPU represents the length of each cable. Fig. 1 presents the CDWP, while Fig. 2 presents its kinematic diagram. The mechanism consists of two platforms, the base and the moving platforms, represented by the letters A and B, respectively. The center of the base platform is at point A_o, while the points A_i represent the position of the proximal anchor points. The following expression presents the values for A_i relative to A_o:

$$A_i = \begin{bmatrix} R_a \cos\alpha_i \\ R_a \sin\alpha_i \\ 0 \end{bmatrix}, \text{ for } \alpha_i = -\frac{\pi}{6} + (i-1)\frac{2\pi}{3} \tag{1}$$

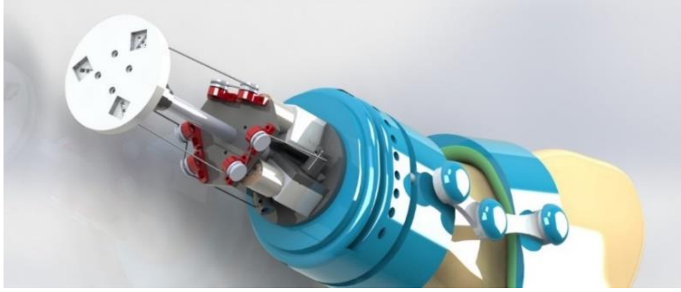

Fig. 1: Cable-driven wrist Prosthesis

Where R_a is the radius of a circumscribed circle around the triangle formed by all the A_i points. At the center of the universal joint attached to the platform is point B_o, while the points B_i represents the position of the distal anchor points. The following expression presents the values for B_i relative to B_o:

$$B_i = \begin{bmatrix} R_b \cos\alpha_i \\ R_b \sin\alpha_i \\ h_b \end{bmatrix}, \text{ for } \alpha_i = -\frac{\pi}{6} + (i-1)\frac{2\pi}{3} \tag{2}$$

Where R_b is the radius of a circumscribed circle around the triangle formed by points B_i. The B_i points share a common plane, let h_b represents the normal distance between this plane and the universal joint. The origin of the global coordinate system is at point A_o, with the x axis in the direction A_o to A_2; The z axis in the direction A_o to B_o; and the y axis is obtained from the cross product of $z \times x$. The position of point B_o relative to point A_o is given by a displacement h in the z axis. At point B_o lies the coordinate system that describes the orientation of the moving platform B, with the $\hat{x}_b$ axis in the direction B'_o to B_2. Where:

$$B'_0 = B_0 + h_b \hat{z}_b$$

$\hat{z}_b$ is the vector normal to the moving platform B. The $\hat{y}_b$ axis obtained from the cross product of $\hat{z}_b \times \hat{x}_b$.

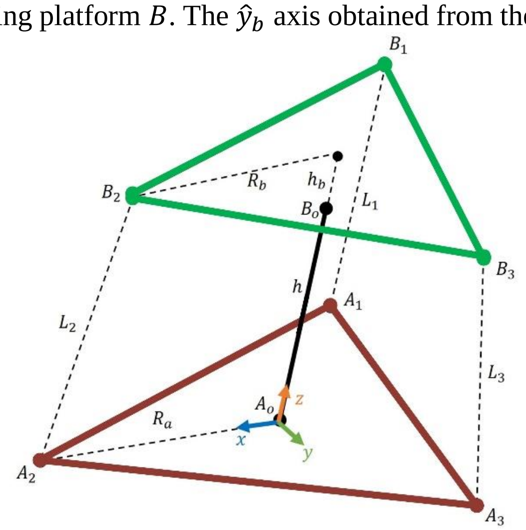

Fig. 2: Kinematic diagram of the proposed cable-driven wrist mechanism

2.1. Inverse kinematics

The inverse kinematics is the equation that expresses the length of the cables as a function of the orientation of the moving platform. To obtain the inverse kinematics, the cable loop equation as presented in the following equation is used:

$${}^{o}A_i - L_i \hat{s}_i = {}^{o}B_i \tag{3}$$

Where the left super-index o represents the values of A_i and B_i in the global coordinate system. The unitary vector $\hat{s}_i$ represents the direction that goes from ${}^{o}B_i$ to ${}^{o}A_i$. To find the length of the links from Eqs. (3) , note that the moving platform B is a rigid body. Therefore, the position of point ${}^{b}B_i$ relative to the moving platform is constant. Besides, the values of ${}^{b}B_i$ are expressed in Eqs. (2). Thus, considering two rotation about the $\hat{x}_b$ and $\hat{y}_b$ axis of the moving platform B by an angle θ_x and θ_y, respectively, the following relation for the points ${}^{o}B_i$ holds:

$$^{o}B_i = R\ ^{b}B_i + \vec{h} \tag{4}$$

Where the matrix R represents two rotations of the moving platform, one in the x-axis, and the other in the y-axis, using rotation matrices. The vector $^{b}B_i$ represents the position of B_i in the coordinate system of the moving platform B. The vector $\vec{h}$ represents the position of B_o with respect to A_o, as follows:

$$\vec{h} = \begin{bmatrix} 0 \\ 0 \\ h \end{bmatrix} \tag{5}$$

Thus, solving Eqs. (3) for L_i and performing the dot product of the result with itself, the solution for L_i is obtained in the following:

$$L_i = \sqrt{\Delta L_{xi}^2 + \Delta L_{yi}^2 + \Delta L_{zi}^2} \tag{6}$$

Where the terms ΔL_{xi}, ΔL_{yi}, and ΔL_{zi} are presented as follows:

$$\begin{aligned} \Delta L_{xi} &= \mathrm{R_a}\cos(\alpha_\mathrm{i}) - \mathrm{R_b}\cos(\alpha_\mathrm{i})\cos(\theta_\mathrm{y}) - \mathrm{h_b}\cos(\theta_\mathrm{x})\sin(\theta_\mathrm{y}) - \mathrm{R_b}\sin(\alpha_\mathrm{i})\sin(\theta_\mathrm{x})\sin(\theta_\mathrm{y}) \\ \Delta L_{yi} &= \mathrm{R_a}\sin(\alpha_\mathrm{i}) + \mathrm{h_b}\sin(\theta_\mathrm{x}) - \mathrm{R_b}\sin(\alpha_\mathrm{i})\cos(\theta_\mathrm{x}) \\ \Delta L_{zi} &= \mathrm{R_b}\cos(\alpha_\mathrm{i})\sin(\theta_\mathrm{y}) - h - \mathrm{h_b}\cos(\theta_\mathrm{x})\cos(\theta_\mathrm{y}) - \mathrm{R_b}\sin(\alpha_\mathrm{i})\cos(\theta_\mathrm{y})\sin(\theta_\mathrm{x}) \end{aligned} \tag{7}$$

3. Objective function

3.1. Anti-parallel based local transmission Index (APLTI)

To determine the objective function, the APLTI is proposed. To define this index, a cable-driven parallel robot with motion in the $\hat{x}\hat{y}\hat{z}$ directions. Each tension acting on the moving platform is represented by a unitary vector $\hat{T}_i$, with each unitary vector pointing to the position of the distal anchor points. Then, assume that it is desirable to know if it is possible to transmit forces acting on the moving platform to the $\hat{x}$ direction for a particular position. Thus, to verify this statement, the following equation is proposed:

$$\mathcal{T}_{\hat{x}} = \hat{T}\ 1\!\upharpoonleft \hat{x} + \hat{T}\ 1\!\downharpoonleft \hat{x} \tag{8}$$

Where $\hat{T}$ is a matrix that contains all the unitary tensions acting on the moving platform, as presented in the following equation:

$$\hat{T} = [\hat{T}_1 \quad \hat{T}_2 \quad \dots \quad \hat{T}_\mathrm{n}] \tag{9}$$

Where n is the total number of cables. The expression $T\ 1\!\upharpoonleft \hat{x}$ is the norm of the positive or parallel projection of the tensions in the $\hat{x}$ direction, as expressed in the following equation:

$$\hat{T}\ 1\!\upharpoonleft \hat{x} = \begin{cases} \left(\sum ((\hat{T}_i \bullet \hat{x})^+)^2\right)^{\frac{1}{2}} & if \quad \left(\sum ((\hat{T}_i \bullet \hat{x})^+)^2\right)^{\frac{1}{2}} < 1 \\ 1 & if \quad \left(\sum ((\hat{T}_i \bullet \hat{x})^+)^2\right)^{\frac{1}{2}} \geq 1 \\ 0 & if \quad \left(\sum ((\hat{T}_i \bullet \hat{x})^-)^2\right)^{\frac{1}{2}} = 0 \end{cases} \tag{10}$$

Where the $+$ sign stands for positive or parallel projection, while the $-$ sign stands for the negative or anti-parallel projection. Similarly, the term $T\ 1\!\downharpoonleft \hat{x}$ is expressed in the following equation:

$$\hat{T}\upharpoonleft\downharpoonright\hat{x} = \begin{cases} \left(\sum\left((\hat{T}_i \bullet \hat{x})^-\right)^2\right)^{\frac{1}{2}} & if \ \left(\sum\left((\hat{T}_i \bullet \hat{x})^-\right)^2\right)^{\frac{1}{2}} < 1 \\ 1 & if \ \left(\sum\left((\hat{T}_i \bullet \hat{x})^-\right)^2\right)^{\frac{1}{2}} \geq 1 \\ 0 & if \ \left(\sum\left((\hat{T}_i \bullet \hat{x})^+\right)^2\right)^{\frac{1}{2}} = 0 \end{cases} \quad (11)$$

This definition is also valid for the $\hat{y}$, and $\hat{z}$ directions. Thus, the APLTI for a cable-driven mechanism is obtained by the following expression:

$$\zeta_{APLTI} = \min(\hat{\mathcal{T}}_{\hat{x}}, \hat{\mathcal{T}}_{\hat{y}}, \hat{\mathcal{T}}_{\hat{z}}) \quad (12)$$

The range of the APLTI is $[0,1]$. Where a value of 0 implies that the motors cannot transmit force to at least one of the directions of motion of the CDPR, in this case, the system is in a singular configuration. Otherwise, a value of 1 implies that by the actuation of one or various motors, the system can generate a force bigger or equal to the higher force transmitted by one motor in each direction of motion of the robot, in this case, the system is in an isotropic configuration. Note that the results for the APLTI are easily extendable to rotations in multiple orthogonal directions. Thus, consider the following expression for a rotation about the $\hat{x}$ direction:

$$\hat{\Psi}_{\hat{x}} = \frac{\hat{\tau}\upharpoonleft\upharpoonright\hat{x} + \hat{\tau}\upharpoonleft\downharpoonright\hat{x}}{2} \quad (13)$$

Where $\hat{\tau}$ is a vector that contains all the torques generated by the unitary tensions acting on the moving platform, as presented in the following equation:

$$\hat{\tau} = \begin{bmatrix} \frac{r_1 \times \hat{T}_1}{\max(r)} & \frac{r_2 \times \hat{T}_2}{\max(r)} & \dots & \frac{r_8 \times \hat{T}_8}{\max(r)} \end{bmatrix} \quad (14)$$

Where r_i is a vector that goes from the center of the moving platform until the distal anchor point corresponding to the unitary tension $\hat{T}_i$. r is a vector that contains the magnitudes of each vector r_i as presented in the following equation:

$$r = [\| r_1 \| \quad \| r_2 \| \quad \dots \quad \| r_n \|] \quad (15)$$

Thus, in the present of rotations, using Eqs. (10), (11), and (13), Eqs. (12) is modified to include the rotation about the $\hat{x}\hat{y}\hat{z}$ directions, as follows:

$$\zeta_{APLTI} = \min\left(\hat{\mathcal{T}}_{\hat{x}}, \hat{\mathcal{T}}_{\hat{y}}, \hat{\mathcal{T}}_{\hat{z}}, \hat{\Psi}_{\hat{x}}, \hat{\Psi}_{\hat{y}}, \hat{\Psi}_{\hat{z}}\right) \quad (16)$$

3.2. Anti-parallel based local transmission Index (APLTI)

To apply Eqs. (16) on the wrist mechanism, consider that the moving platform is attached to a universal joint. Then, since the universal joint allows independent rotations in two directions, the tensions acting on it generates two torques in the $\hat{x}$ and $\hat{y}$ directions. Therefore, the vector $\hat{\tau}$ of the wrist mechanism is presented in the following equation:

$$\hat{\tau} = \begin{bmatrix} \frac{{}^oB_1 \times \hat{s}_1}{\|{}^oB_1\|} & \frac{{}^oB_2 \times \hat{s}_2}{\|{}^oB_2\|} & \frac{{}^oB_3 \times \hat{s}_3}{\|{}^oB_3\|} \end{bmatrix} \quad (17)$$

Note that the term ${}^{o}B_i$, as defined in Eqs 4, is equivalent to r_i. Besides, since the term $\hat{s}_i$ is a unitary vector pointing in the direction of the i cable, $\hat{s}_i$ is equivalent to $\hat{T}_i$, then, the following equation expresses the value of $\hat{s}_i$ obtained by solving Eqs. (3):

$$\hat{s}_i = \frac{{}^{o}A_i - {}^{o}B_i}{L_i} \tag{18}$$

Additionally, the following relation holds for the terms $\|{}^{o}\ B_i\ \|$:

$$\|{}^{o}\ B_1\ \| = \|{}^{o}\ B_2\ \| = \|{}^{o}\ B_3\ \| = \sqrt{R_b^2 + h_b^2} \tag{19}$$

Thus, the following equation is used for the calculation of the APLTI for the CDWP:

$$\zeta_{APLTI} = \min\left(\widehat{\Psi}_{\hat{x}}, \widehat{\Psi}_{\hat{y}}\right) \tag{20}$$

3.3. Anti-parallel based local transmission Index (APLTI)

The calculation of the Global anti-parallel transmission index (GAPTI) considers the distribution of APLTI in the workspace of the CDWP. A popular tool to find the distribution of an index in the workspace is the mean of a function [29], defined in the following equation:

$$\Xi_{GAPTI} = \frac{\sum_{i=1}^{v} \sum_{i=1}^{w} \zeta_{APLTI}(\theta_{xi}, \theta_{yj})}{vw} \tag{21}$$

Note that the workspace of the CDWP is defined by two rotations, one about the $\hat{x}$ direction and the other about the $\hat{y}$ direction. Thus, the workspace was subdivided in differentials $d\theta_x$ and $d\theta_y$. Then, u and v are the total number of partions of $d\theta_x$ and $d\theta_y$. Lastly, Eqs. (21) is the objective function for the optimization of the CDWP.

5. Optimization of the CDWP

In the following, an GA [21] is implemented to optimize the design of the CDWP. Table 1 presents the minimum, maximum, and optimum of the optimization variables.

Table 1. Minimum, maximum, and optimum of the optimization variables in mm.

	Minimum	Maximum	Optimum
$\boldsymbol{R_a}$	22	42	30.70559
$\boldsymbol{R_b}$	19	40	40
$\boldsymbol{h}$	50	120	120
$\boldsymbol{h_b}$	13	22	19

Note that, for the calculation of Ξ_{GAPTI}, we considered that each orientation θ_x and θ_y moves within the interval $(-70^{o}, 70^{o})$. This interval was obtained from considering the workspace spanned by the human wrist [30]. The evolution of the objective function along generations is presented in Fig. 3. As can be seen, the optimization reached its maximum value around the 100 generation. Thus, the maximum values of Ξ_{GAPTI} is 0.7544.

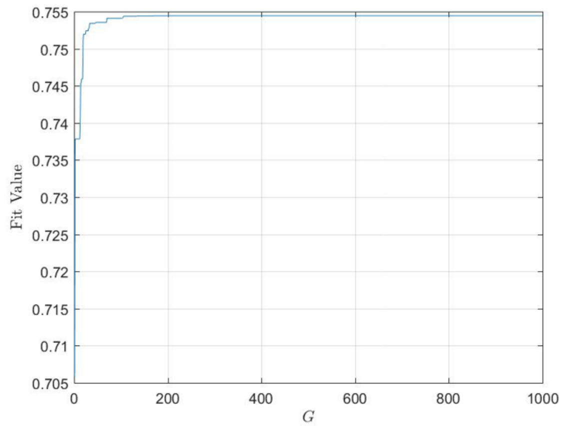

Fig. 3: Evolution of the objective function along the generations of the GA.

The distribution of the index within the workspace is presented in Fig. 4. Both the maximum and minimum values of the ζ_{APLTI} are 0.7959 and 0.6686, which are located at the configuration $(15.94^{o}, -52.8113^{o})$ and $(-70^{o}, -70^{o})$, respectively.

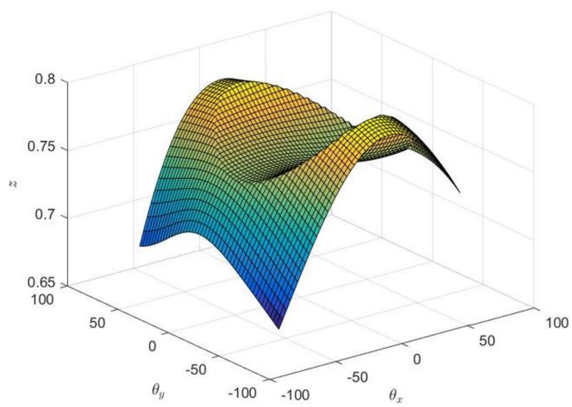

Fig. 4: Distribution of ζ_{APLTI}

6. Conclusion

In this research, the optimal design of a CDWP is presented. To conduct the design, a performance index called the APLTI is proposed. This index allowed us to know the relation between the transmission of the torque or forces on a parallel robot. Then, by the application of genetic algorithms, the CDWP is optimized. Thus, the two main contributions of this research are the implementation of a methodology that allows the dimensioning of an easy to manufacture prosthesis for upper limb amputees and the definition of a performance index that allows the fast dimensioning of CDPR for diverse applications.

Acknowledgments

With our deepest gratitude, the authors acknowledge the support of Luis Jose Hernandez De Caro, long rest to his soul.

References

[1] E. National Academies of Sciences, Engineering, and Medicine, "Upper-Extremity Prostheses," in *The Promise of Assistive Technology to Enhance Activity and Work Participation*: National Academies Press (US), 2017.

[2] Sunny, M. S. H., Zarif, M. I. I., Rulik, I., Sanjuan, J., Rahman, M. H., Ahamed, S. I., Wang I, Schultz K., & Brahmi, B.., "Eye-gaze control of a wheelchair mounted 6DOF assistive robot for activities of daily living," (in eng), *J Neuroeng Rehabil*, vol. 18, no. 1, p. 173, Dec 18 2021.

[3] K. Ziegler-Graham, E. J. MacKenzie, P. L. Ephraim, T. G. Travison, and R. Brookmeyer, "Estimating the Prevalence of Limb Loss in the United States: 2005 to 2050," *Archives of Physical Medicine and Rehabilitation,* vol. 89, no. 3, pp. 422-429, 2008/03/01/ 2008.

[4] N. M. Bajaj, A. J. Spiers, and A. M. Dollar, "State of the Art in Artificial Wrists: A Review of Prosthetic and Robotic Wrist Design," *IEEE Transactions on Robotics,* vol. 35, no. 1, pp. 261-277, 2019.

[5] A. G. Mell, B. L. Childress, and R. E. Hughes, "The Effect of Wearing a Wrist Splint on Shoulder Kinematics During Object Manipulation," *Archives of Physical Medicine and Rehabilitation,* vol. 86, no. 8, pp. 1661-1664, 2005/08/01/ 2005.

[6] B. D. Adams, N. M. Grosland, D. M. Murphy, and M. McCullough, "Impact of impaired wrist motion on hand and upper-extremity performance1 1No benefits in any form have been received or will be received from a commercial party related directly or indirectly to the subject of this article," *The Journal of Hand Surgery,* vol. 28, no. 6, pp. 898-903, 2003/11/01/ 2003.

[7] F. Montagnani, M. Controzzi, and C. Cipriani, "Is it Finger or Wrist Dexterity That is Missing in Current Hand Prostheses?," *IEEE Transactions on Neural Systems and Rehabilitation Engineering,* vol. 23, no. 4, pp. 600-609, 2015.

[8] F. Cordella, A. L. Ciancio, R. Sacchetti, A. Davalli, A. G. Cutti, E. Guglielmelli, and L. Zollo, "Literature Review on Needs of Upper Limb Prosthesis Users," (in English), *Frontiers in Neuroscience,* Review vol. 10, no. 209, 2016-May-12 2016.

[9] N. M. Bajaj, A. J. Spiers, and A. M. Dollar, "State of the art in prosthetic wrists: Commercial and research devices," in *2015 IEEE International Conference on Rehabilitation Robotics (ICORR)*, 2015, pp. 331-338.

[10] A. Mutlu, M. D. Kharooty, and Y. Yakut, "The effect of segmental weight of prosthesis on hemodynamic responses and energy expenditure of lower extremity amputees," (in eng), *Journal of physical therapy science,* vol. 29, no. 4, pp. 629-634, 2017.

[11] E. A. Biddiss and T. T. Chau, "Upper limb prosthesis use and abandonment: A survey of the last 25 years," *Prosthetics and Orthotics International,* vol. 31, no. 3, pp. 236-257, 2007.

[12] R. Mahmoud, A. Ueno, and S. Tatsumi, "Dexterous mechanism design for an anthropomorphic artificial hand: Osaka City University Hand I," in *2010 10th IEEE-RAS International Conference on Humanoid Robots*, 2010, pp. 180-185.

[13] G. T. Pinson, "Digitally-controlled artificial hand," 1981.

[14] K. B. Fite, T. J. Withrow, X. Shen, K. W. Wait, J. E. Mitchell, and M. Goldfarb, "A gas-actuated anthropomorphic prosthesis for transhumeral amputees," *IEEE Transactions on Robotics,* vol. 24, no. 1, pp. 159-169, 2008.

[15] S. K. Kundu and K. Kiguchi, "Development of a 5 DOF prosthetic arm for above elbow amputees," in *2008 IEEE International Conference on Mechatronics and Automation*, 2008, pp. 207-212: IEEE.

[16] H. Takeda, N. Tsujiuchi, T. Koizumi, H. Kan, M. Hirano, and Y. Nakamura, "Development of prosthetic arm with pneumatic prosthetic hand and tendon-driven wrist," in *2009 Annual International Conference of the IEEE Engineering in Medicine and Biology Society*, 2009, pp. 5048-5051: IEEE.

[17] M. Controzzi, C. Cipriani, B. Jehenne, M. Donati, and M. C. Carrozza, "Bio-inspired mechanical design of a tendon-driven dexterous prosthetic hand," in *2010 Annual International Conference of the IEEE Engineering in Medicine and Biology*, 2010, pp. 499-502: IEEE.

[18] N. Jarrassé and G. Morel, "Connecting a human limb to an exoskeleton," *IEEE Transactions on Robotics,* vol. 28, no. 3, pp. 697-709, 2011.

[19] Y. Jung and J. Bae, "An asymmetric cable-driven mechanism for force control of exoskeleton systems," *Mechatronics,* vol. 40, pp. 41-50, 2016.

[20] P. Garrec, "Design of an anthropomorphic upper limb exoskeleton actuated by ball-screws and cables," *University" Politehnica" of Bucharest Scientific Bulletin, Series D: Mechanical Engineering,* vol. 72, no. 2, pp. 23-34, 2010.

[21] D. Chiaradia, M. Xiloyannis, C. W. Antuvan, A. Frisoli, and L. Masia, "Design and embedded control of a soft elbow exosuit," in *2018 IEEE International Conference on Soft Robotics (RoboSoft)*, 2018, pp. 565-571: IEEE.

[22] H. I. Krebs and B. T. Volpe, "Robotics: A rehabilitation modality," *Current physical medicine and rehabilitation reports*, vol. 3, no. 4, pp. 243-247, 2015.
[23] S. K. Mustafa and S. K. Agrawal, "On the force-closure analysis of n-DOF cable-driven open chains based on reciprocal screw theory," *IEEE Transactions on Robotics*, vol. 28, no. 1, pp. 22-31, 2011.
[24] F. Hao and J.-P. Merlet, "Multi-criteria optimal design of parallel manipulators based on interval analysis," *Mechanism and machine theory*, vol. 40, no. 2, pp. 157-171, 2005.
[25] E. Ottaviano and G. Carbone, "A procedure for the multiobjective design of parallel manipulators," *International Journal of Mechanics and Control*, vol. 4, no. 02, pp. 57-62, 2003.
[26] J. Sanjuan, E. Muñoz, M. Padilla, and M. Rahman, "The kinematic effects of simplifications in the analysis of linear translational parallel robots," *International Journal of Dynamics and Control*, 2022/01/15 2022.
[27] G. Carbone, C. A. Cavero, M. Ceccarelli, and O. Altuzarra, "A study of feasibility for a limb exercising device," in *Advances in Italian Mechanism Science*: Springer, 2017, pp. 11-21.
[28] M. A. Laribi, G. Carbone, and S. Zeghloul, "On the optimal design of cable driven parallel robot with a prescribed workspace for upper limb rehabilitation tasks," *Journal of Bionic Engineering*, vol. 16, no. 3, pp. 503-513, 2019.
[29] C. Gosselin and J. Angeles, "A global performance index for the kinematic optimization of robotic manipulators," 1991.
[30] J. D. Sanjuan, A. D. Castillo, M. A. Padilla, M. C. Quintero, E. E. Gutierrez, I. P. Sampayo, J. R. Hernandez, M. H. Rahman "Cable driven exoskeleton for upper-limb rehabilitation: A design review," *Robotics and Autonomous Systems*, vol. 126, p. 103445, 2020.